

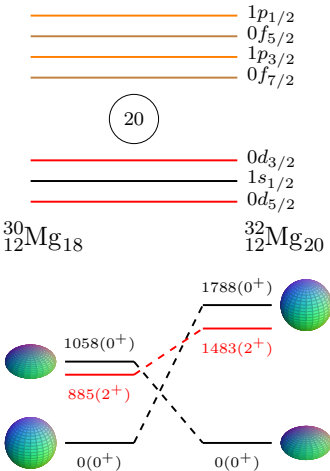
Evolution of single-particle structure along $N = 17$: The $d(^{28}\text{Mg},p)^{29}\text{Mg}$ reaction measured with the ISOLDE Solenoidal Spectrometer

Patrick MacGregor
ISOLDE Workshop and Users meeting 2020
26 November 2020



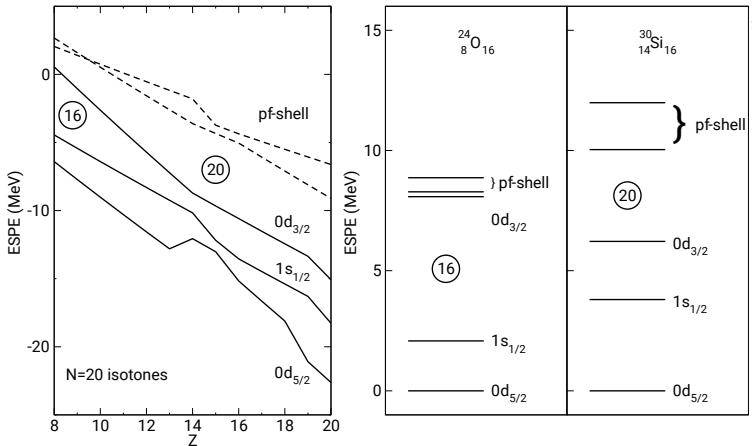
Motivation – approaching $N = 20$ island of inversion

- There is an island of inversion around $N = 20$ for exotic nuclei.
- Defined by “intruder configurations” in ground state and low-lying excited states, where neutrons are promoted across shell gaps, leaving neutron holes.
- Evidenced by observation of many negative-parity states at low excitation energies.
- Sharp transition in isotopes of Mg:
 - ^{30}Mg outside the island → spherical g.s.
 - ^{32}Mg inside the island → deformed g.s.¹.
- Measurement of single-particle properties crucial for understanding shell evolution in and around the island.
- ^{29}Mg outside the island, but mapping the size of shell gaps crucial for understanding this region.

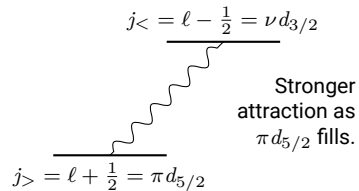


¹ K. Wimmer et al. *Phys. Rev. Lett.* 105 (Dec. 2010), p. 252501.

Motivation – $N = 20$ shell gap evolution



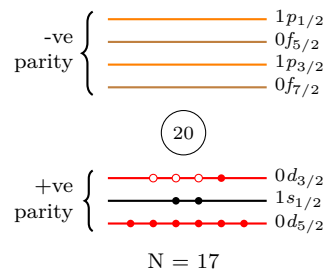
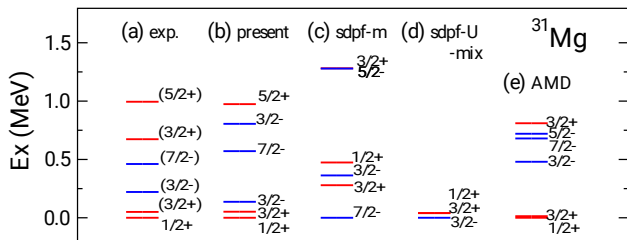
- Observed weakening in the $N = 20$ shell closure with decreasing Z .
- Weakening caused by relative strength of interaction between neutrons and protons in different orbits ($\nu d_{3/2}, f_{7/2}, p$ and $\pi d_{5/2}$). Orbitals experience different monopole shifts.
- Transfer reactions can be used here to map evolution of p f-states and how separation evolves.



² Adapted from T. Otsuka et al. Eur. Phys. J. A. 15 (2002), pp. 151–155.

Motivation – new shell model interactions

- Standard shell model calculations fail to reproduce experimental data without ad hoc changes.
- A number of interactions developed for the *sdpf*-model space:
 - SDPF-MU³, a more established interaction, that uses 0p-0h and 1p-1h excitations for positive and negative parity states respectively, and is fitted to experimental data in this region.
 - FSU interaction⁴, similar to SDPF-MU, but fits more TBMEs and SPEs in this particular region.
 - EEdf1⁵uses chiral EFT + extended Kuo-Krenciglowa (EKK) method to calculate over multiple major oscillator shells. Also uses 3-body interactions to model nuclei. Shown below for ³¹Mg.
- RMS deviation approx. 300 keV better for FSU and EEdf1 than SDPF-MU.

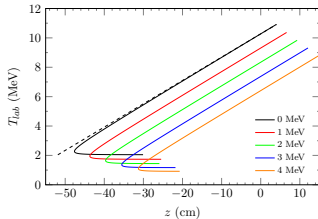


³ Y. Utsuno. Priv. communication.

⁴ R. Lubna. Priv. communication.

⁵ N. Tsunoda et al. Phys. Rev. C 95 (2 Feb. 2017), p. 021304.

Solenoidal spectrometers



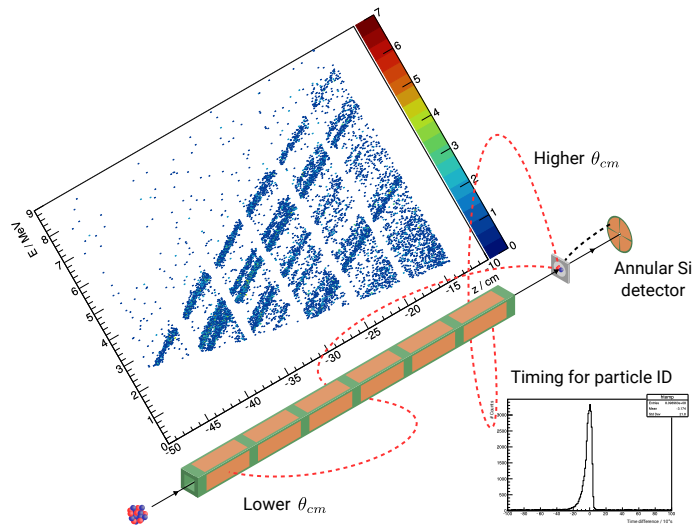
Measure z rather than θ .

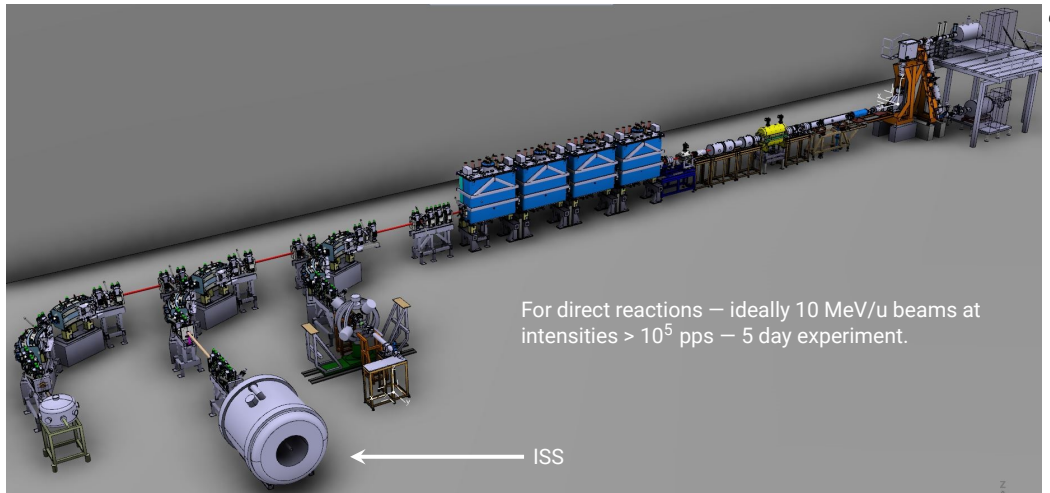
For a given z , $T_{lab} \propto \Delta E_x$.
⇒ no compression in the solenoid.

⇒ better resolution.

"Knees" introduced as a result of finite array size.

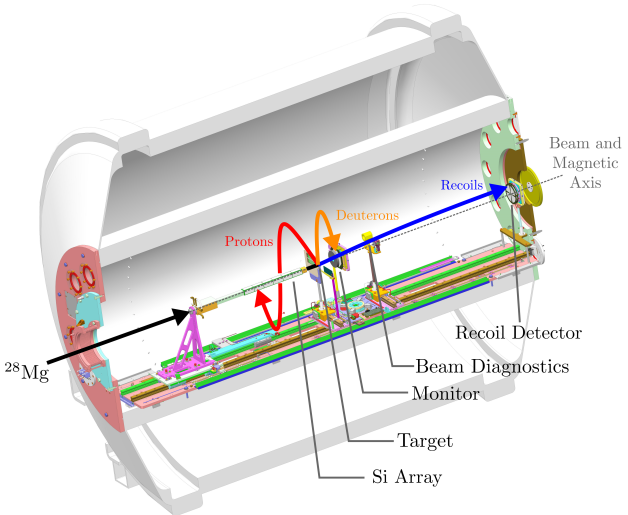
$$T_{lab} = T_{cm} - \frac{1}{2}mv_{cm}^2 + \frac{mv_{cm}z}{t_{cyc}}$$





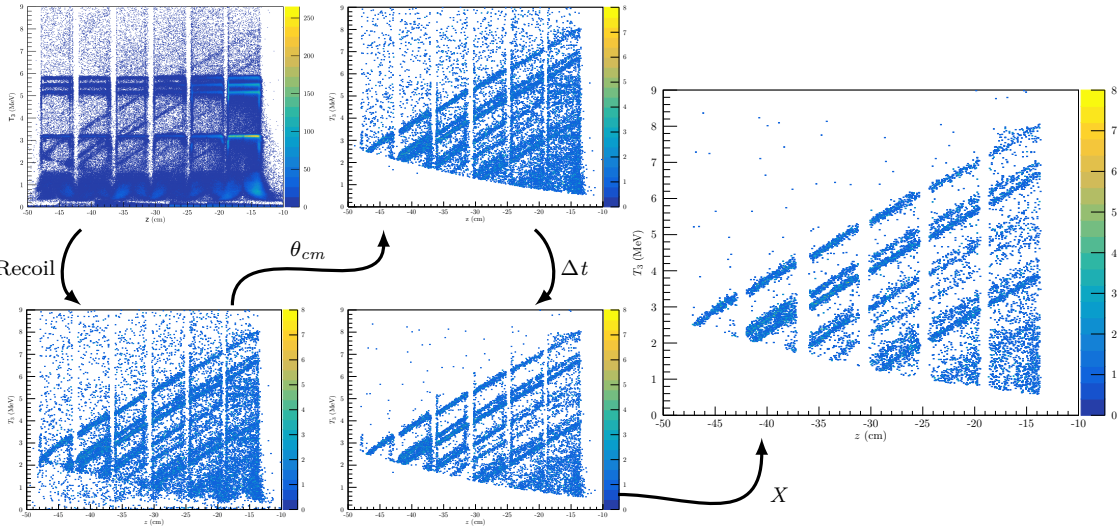
⁶ URL: <http://hie-isolde-project.web.cern.ch/about-hie-isolde>.

ISS Setup

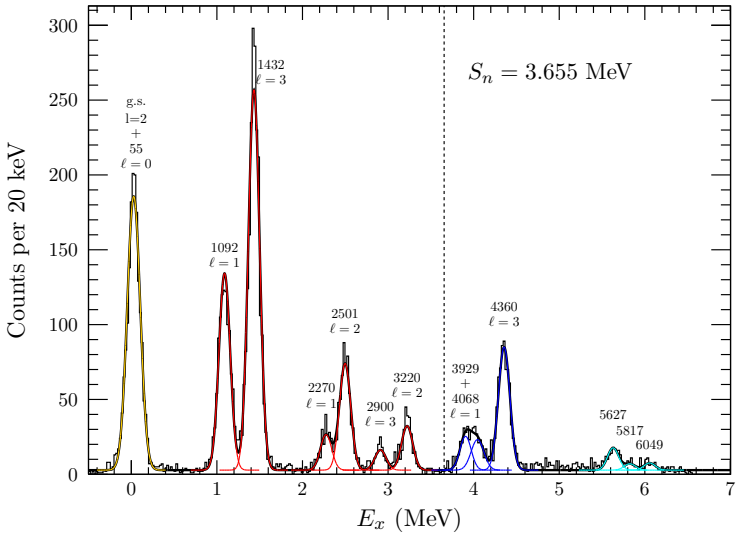


- Based on HELIOS spectrometer at Argonne National Laboratory.
- Detectors:
 - HELIOS array – backwards scattered p .
 - S1 detector – elastically scattered d .
 - $E\Delta E$ recoil detector – scattered beam.
- Measure energy signals and timestamps on each detector.
- Beam energy: 9.473 MeV/u ($dE/E = 0.3\%$).
- Maximum 10^6 pps.

Analysis methodology

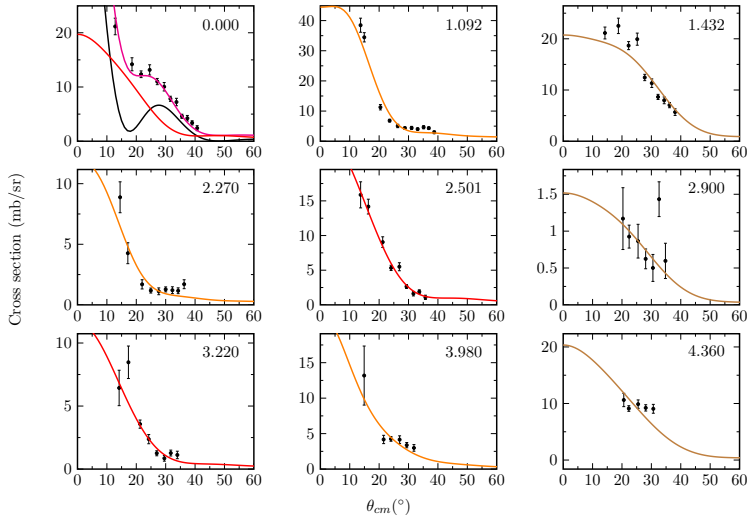


Results – excitation spectrum



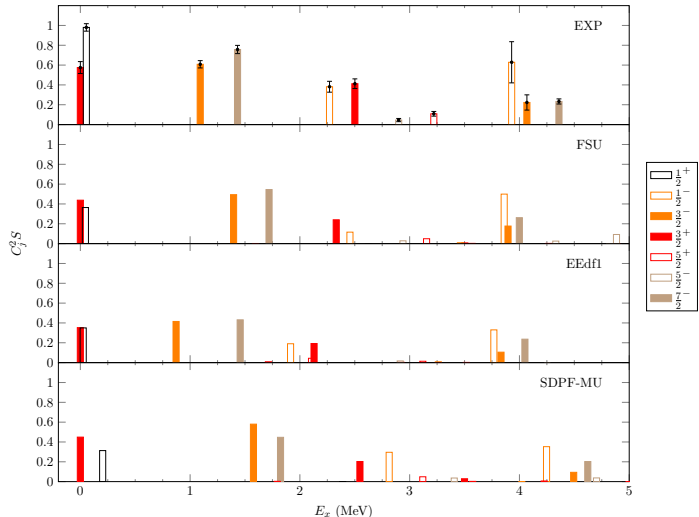
- Identified 14 states in ^{29}Mg .
- Resolved 2270, 2501, 2900, and 3220 keV states and able to assign ℓ .
- Identified a number of unbound states, including a doublet $\ell = 1$ state and some high-excitation weaker states.
- Extracted cross sections at different angles for $7 + 2$ doublets.

Results – cross sections



- Fitted cross sections using DWBA angular distributions from DWUCK5.
- Able to assign ℓ from the angular distributions.
- State labelled 3.980 MeV is the unbound doublet.

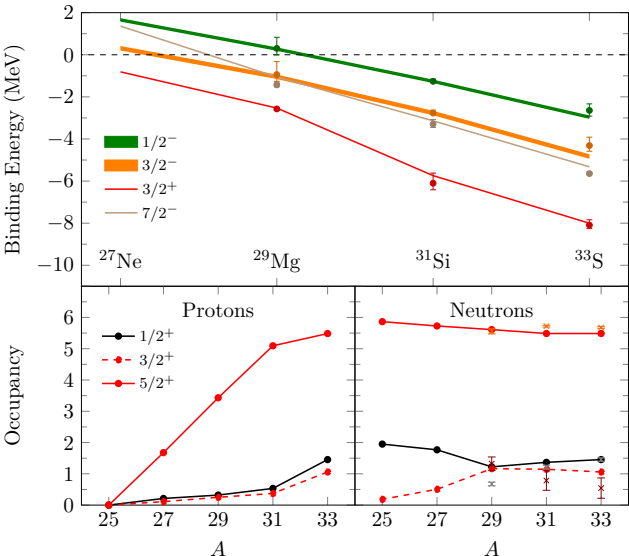
Results – spectroscopic factors



- Can tentatively assign j^π for experimental results from shell-model calculations.
- Reasonable agreement for the distribution of strength in strong states.
- Inform most likely ordering of j^π for doublet state.

Results – shell evolution

- Plotted centroids of single-particle strength in terms of binding energy for theoretical and experimental^{7,8,9} results (relative to ^{31}Si). Error bars include ambiguities in j -assignment.
- As calculations reproduce trends reasonably well, plotted occupancies from the same model for protons and neutrons.
- Normalised SFs from experimental papers and calculated occupancies for comparison. Discrepancies in ^{29}Mg possibly due to g.s. doublet fit, or a change in neutron occupancies.
- Measurement of ($d, ^3\text{He}$) needed to confirm expected proton occupancies.



⁷ Š. Piskor et al. *Nucl. Phys. A* 662.1 (2000), pp. 112–124.

⁸ M. C. Mermaz et al. *Phys. Rev. C* 4 (5 Nov. 1971), pp. 1778–1800.

⁹ R. Liljestrand et al. *Phys. Rev. C* 11 (5 May 1975), pp. 1570–1577.

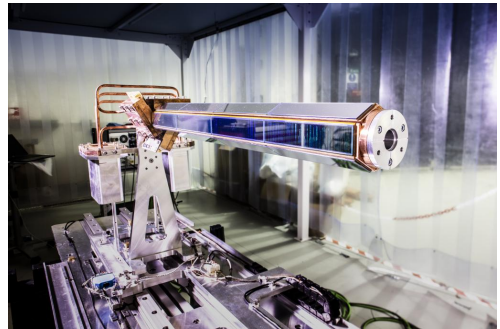
Conclusions and future

Conclusions:

- First experiment of ISS in early implementation stage.
- Comparable resolution to HELIOS.
- Highest energy per nucleon in a HIE-ISOLDE radioactive beam experiment.
- A successful experiment!

Future:

- $^{29}\text{Al}(d,p)$ experiment recently performed at HELIOS – more information for this region.
- Hoping to get $^{30}\text{Mg}(d,p)$ data from ISS in future.
- Bright future for ISS - Liverpool array, SpecMAT.



Acknowledgements

Manchester Group

D. K. Sharp
B. D. Cropper

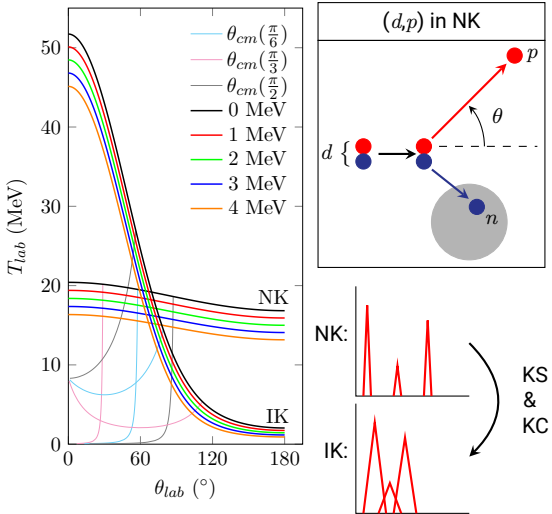
S. J. Freeman

Additional Collaborators

C. R. Hoffman
L. P. Gaffney
M. Borge
W. N. Catford
J. Konki
M. Labiche
I. Martel
R. D. Page
R. Raabe
T. L. Tang

B. P. Kay
E. F. Baader
P. A. Butler
G. de Angelis
Th. Kröll
I. H. Lazarus
D. G. McNeil
O. Poleshchuk
F. Recchia
J. Yang

Transfer reactions in inverse kinematics



- Ejectile, p , provides information for the populated state in ^{29}Mg :
 - Yields → cross section.
 - θ → angular momentum.
 - Ejectile energy → excitation of residual nucleus.
- Single-particle strength split by correlations between nucleons.
- Deduce spectroscopic factors, $S_{j\ell}$, which measure how close each state looks like a n in IPM state:

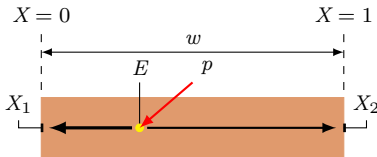
$$\left(\frac{d\sigma}{d\Omega} \right)_{\text{EXP}} = S_{j\ell} \left(\frac{d\sigma}{d\Omega} \right)_{\text{DWBA}}$$

where $|^{29}\text{Mg}; j, \ell \rangle \sim \sum_{j,\ell} S_{j\ell} (|^{28}\text{Mg}; 0, 0 \rangle \otimes |n; j, \ell \rangle)$.

- $^{28}\text{Mg} \rightarrow ^{28}\text{Al}$ via β^- ; $\tau_{1/2} = 21 \text{ h}$. NK not possible, so use IK.
- IK allows transfer on radioactive nuclei, but introduces some non-trivial problems:
 1. Kinematic shift (KS) - broadens peaks because of large $\frac{dE}{d\theta}$ for a finite angular acceptance, $\Delta\theta$.
 2. Kinematic compression (KC) reduces energy difference between states.

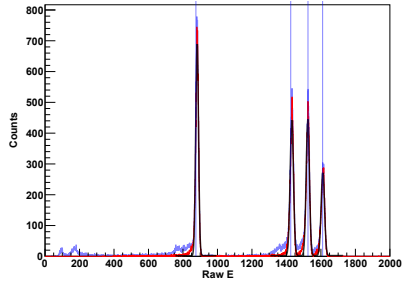
Extracting E and z

Positions:



$$\text{Position on strip} = X = \begin{cases} 1 - \frac{X_1}{E}, & X_1 > 0.5E \\ \frac{X_2}{E}, & X_2 > 0.5E \end{cases}$$

Energies:



- Calculate position on strip using gain-matched X_1 , X_2 , and E .
- Use laser alignment from CERN team to calculate distance from target:

$$z = \left(X - \frac{1}{2} \right) w - z_{\text{off}} - d_i.$$

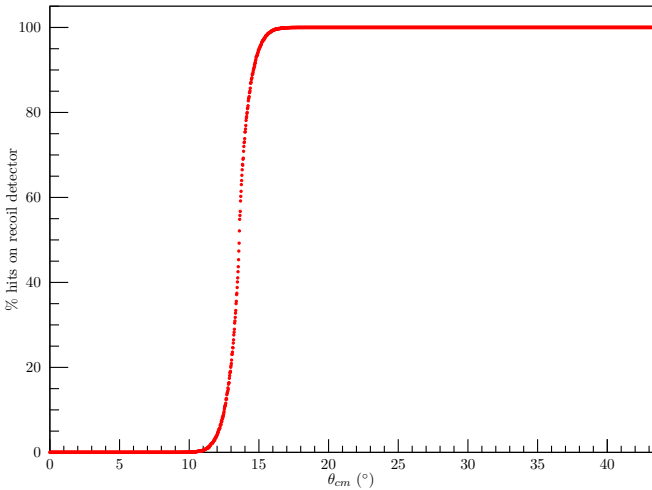
z is the distance along the beam axis from the target.

d_i is the distance along the array to the centre of strip i .

z_{off} is the distance from the target to the array.

- Gain match X_1 and X_2 to each other.
- Match X_1 and X_2 to E .
- Rough energy calibration with quadruple α -source.
- α -source not sufficient for full calibration, as α 's lose energy in the target.
- α -source calibration improved by calibrating to known states in ^{29}Mg .

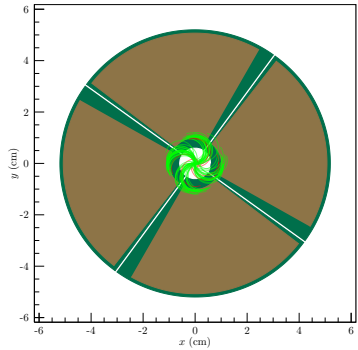
Further analysis – recoil-proton coincidences



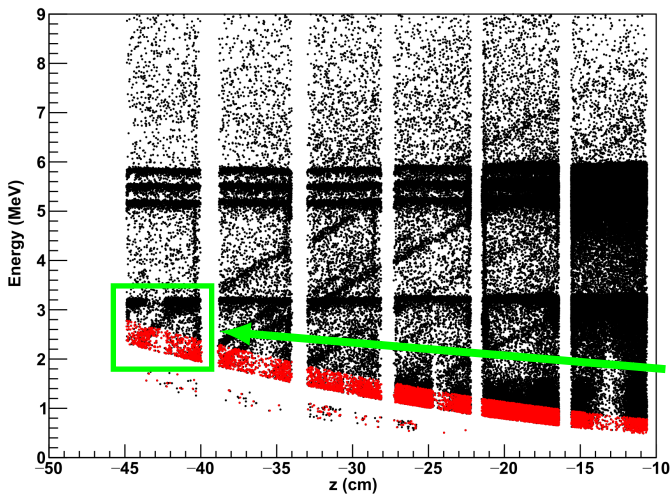
Simulated number of recoiling nuclei hitting the recoil detector (at ≈ 4.3 MeV).

\Rightarrow some recoiling nuclei don't hit the recoil detector.

\Rightarrow low-angle points impossible to obtain based on cuts.



Further analysis – recoil-proton coincidences



Simulated number of recoiling nuclei hitting the recoil detector (at ≈ 4.3 MeV).

⇒ some recoiling nuclei don't hit the recoil detector.

⇒ low-angle points impossible to obtain based on cuts.

Solution:

Use careful θ_{cm} cuts on the singles data to extract low-angle points.

Can see that the angle cuts here don't include α -line in first row, but do include low-angle points for the ground state.